Haze and Fog Aerosol Distributions[1,2]

RALPH G. ELDRIDGE
The MITRE Corporation, Bedford, Mass.

(Manuscript received 4 November 1965, in revised form 1 April 1966)

ABSTRACT

Spectral attenuation measurements through haze and fogs are used to synthesize aerosol distributions characteristic of the attenuating medium. Twelve fog drop-size distributions have been averaged into two general types of fogs for comparison with measured fog drop-size distributions and with a distribution predicted by theory. Seven time-phased fog drop-size distributions are used to illustrate the phenomena of droplet growth and fog degeneration. Finally, an empirical relationship between liquid water content and visual range is presented.

1. Introduction

Some years ago Arnulf *et al.* (1957) published the results of a series of spectral optical density measurements through haze and fogs. Prior to this, Eldridge (1957a) had published some cloud drop-size distributions inferred from spectral attenuation measurements. Briefly, the method used by Eldridge consists of making successive synthetic droplet distributions and comparing the resulting spectral attenuations with those measured experimentally. When the two spectral attenuations are similar, then the synthetic distribution is considered to be representative of that causing the measured spectral attenuation. The attendant problems of this numerical integration technique have been discussed by Penndorf (1957) and Eldridge (1957b). Although there remains a theoretical doubt as to the uniqueness of the inferred distribution, the practical application of this technique merits further consideration, especially with the excellent data of Arnulf *et al.*

Measured spectral attenuations (Arnulf *et al.*, 1957) have been used to infer synthetic aerosol distributions for haze and fog. The computed haze aerosol distribution is compared with haze models (Junge, 1955) and a measured haze aerosol distribution (Arnulf *et al.*, 1957). The computed fog drop-size distributions are compared with fog distributions measured with the "spider web" technique (Arnulf *et al.*, 1957) and with drop-size distributions predicted by droplet growth theory (Neiburger and Chien, 1960).

The aerosol distributions which follow are in the size range from about 0.3 to 10 μ radius. This size range is generally considered to span aerosols described as haze particles and smaller cloud or fog droplets. This size range also includes those haze particles capable of growing into fog or cloud droplets when subjected to the proper environment. The aerosol distributions are referred to as haze or fog distributions, not because of the size range of aerosols, but rather as an indication of the meteorological conditions prevailing at the time of the spectral attenuation measurements. The fog aerosol distributions suggest some similarities with haze distributions in the sub-micron size region, but there is considerable dissimilarity in the size range larger than a micron.

2. Haze aerosol distributions

The measured spectral attenuation of visible and infrared radiation by haze is summarized in three curves by Arnulf *et al.*, in Fig. 6 of their paper. Because these curves are similar in shape and magnitude, they are averaged for analysis. Spectral attenuations are computed by generating a synthetic distribution of aerosols and computing the attenuation coefficient σ_λ for each wavelength, where

$$\sigma_\lambda = 2\pi N \sum^{i} (N_i/N) K_{\lambda i} r_i^2. \quad (1)$$

The total number of aerosols in the distribution is N, while N_i is the number of aerosols of size r_i, which is the mean radius of aerosols in class i. The scattering cross section $K_{\lambda i}$ is a consequence of Mie scattering principles. The assumption is made that haze aerosols are composed of nuclei which are sufficiently hygroscopic to acquire a coating of water, and therefore, they scatter essentially in the same manner as water droplets. This allows the use of scattering cross sections published by Johnson and Terrell (1955) for the complex index of refraction for water aerosols illuminated by infrared radiation, and the use of the scattering cross sections published by Houghton and Chalker (1949) for the visible region of the spectrum. The use of an index of refraction of 1.33 for haze aerosols is convenient, though not necessarily the most appropriate. However, the investigation of Gibbons (1958) indicates (see his Fig. 1) that for values of the size parameter $\alpha = 2\pi r/\lambda$ from 3 to

[1] The research reported was partially sponsored by the Electronic Systems Division, Air Force Systems Command under Contract Number AF19(628)5165. This paper will also be available as ESD-TR-113. Further reproduction is authorized to satisfy the needs of the U. S. Government.

[2] The substance of this paper was presented at the 244th National Meeting of the American Meteorological Society on Cloud Physics and Severe Local Storms, 18–22 October 1965, Reno, Nev.

about 6.5, an index of refraction of 1.33 approximates natural haze more adequately than other values. Therefore, for visible radiation ($\lambda = 0.5 \pm 0.2\,\mu$), the appropriate aerosol size range is from 0.1–0.7 μ radius.

The technique for computing spectral attenuations can be best illustrated by generating a synthetic aerosol distribution characteristic of haze. Eq. (1) is used to compute the spectral attenuations which are then normalized at one wavelength. By successive and judicious selections of concentrations and of aerosol sizes, a spectral attenuation is computed which approximates the measured spectral attenuation. For example, given the haze spectral attenuation σ_m, and then selecting 550–0.35, 750–0.45 and 20–0.75 μ radius aerosols, a computed spectral attenuation σ_c results. This is tabulated below for comparison with the measured spectral attenuation

λ	0.35	0.385	0.45	0.50	0.55	0.75	1.24	1.70	3.7	9.5
σ_m	3.28	3.68	3.57	3.48	3.30	2.54	0.97	0.62	0.32	0.19
σ_c	3.38	3.49	3.63	3.49	3.30	2.33	0.91	0.41	0.08	0.00

σ_m. Comparison of σ_m and σ_c at all wavelengths indicates that there is a divergence between the computed and measured spectral attenuations at longer wavelengths. Therefore, it is propitious to add larger aerosols to the distribution. The addition of 0.2 of a droplet in the 8.5- and 9.5-μ radius intervals results in the following spectral attenuation:

λ	0.35	0.384	0.45	0.50	0.55	0.75	1.24	1.70	3.7	9.5
σ_m	3.28	3.68	3.57	3.48	3.30	2.54	0.97	0.62	0.32	0.19
σ_c	3.37	3.48	3.62	3.48	3.30	2.36	0.97	0.48	0.19	0.11

The addition of a fraction of micron size aerosols improves the agreement between the computed and measured spectral attenuations. Therefore, this iterative procedure is continued until the addition or subtraction of any size aerosol in significant numbers causes a divergence of the computed spectral attenuation from the measured spectral attenuation. At this time, the computed spectral attenuation is considered to be the best practical fit to the measured spectral attenuation, and the synthetic distribution approximates that which existed in nature and caused the measured spectral attenuation.

The spectral attenuation resulting from the final synthesized aerosol distribution (Fig. 1) is compared with the measured spectral attenuation in Fig. 2. The synthesized haze aerosol distribution is plotted in Fig. 1 with three haze models published by Junge (1955). The Junge haze models illustrate the growth of haze aerosols in environments of 70, 99 and 100 per cent relative humidities. The fourth curve represents the average of the two haze distributions used by Neiburger and Chien (1960) for their cloud droplet growth study. According to Junge (1957), deviations of an order of magnitude or more in concentration of aerosols do occur in nature. Therefore, it is quite encouraging to note that the synthetic haze distribution, with a visibility computed with Koschmider's formula of about 1.2 km, migrates between the two Junge haze distributions which have computed visibilities of 5.7 and 1.1 km.

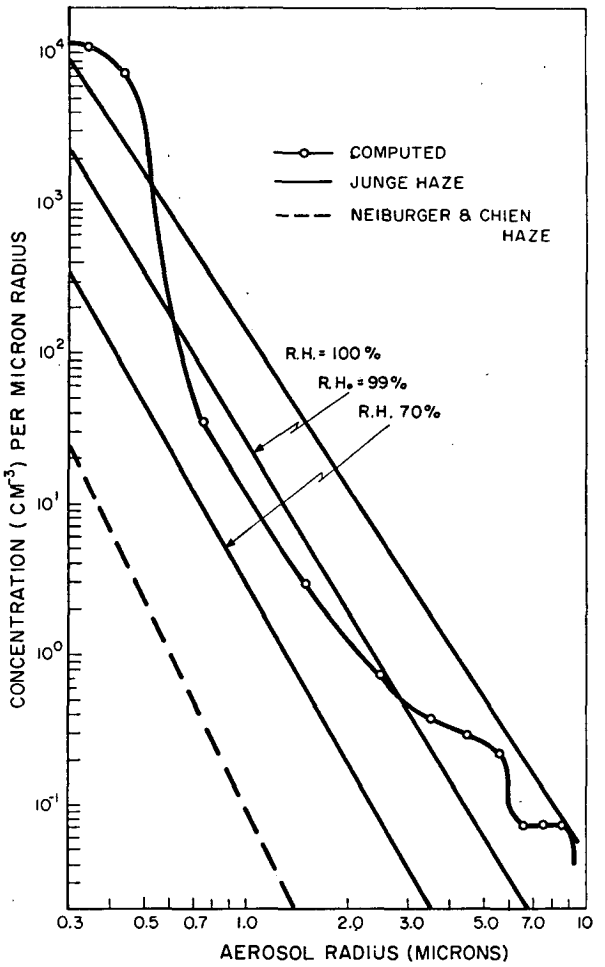

FIG. 1. Comparison of the synthetic haze aerosol distribution with various haze models.

The "goodness of fit," illustrated in Fig. 2, may be expressed in terms of the average deviation of the computed spectral attenuation curve from the measured spectral attenuation curve. The average deviation over the spectral range from 0.35 to 9.5 μ wavelength is 5.0 per cent. The resulting uncertainty in the total number of particles is 128 out of a total of 1890 droplets cm^{-3}, or 6.8 per cent. The maximum uncertainty in the determination of the total number of droplets resulting from the "poorest fit" between the two curves at one wavelength is 340 droplets cm^{-3}, or 18 per cent.

The uncertainty inherent in the computational process may be assessed by independently computing the total number of droplets in the distribution for each wavelength. The mean deviation from the average total number of droplets is 13 per cubic centimeter, or 0.7 per cent. The maximum deviation at the wavelength with the "poorest fit" results in an uncertainty of 35 droplets cm^{-3}, or 1.9 per cent.

In summary, it should be noted that the uncertainties

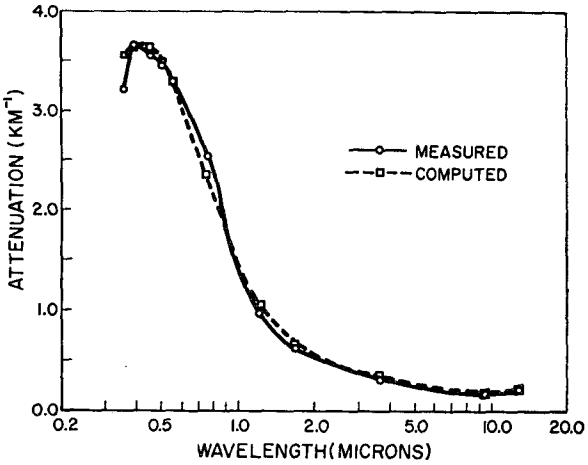

FIG. 2. Measured and computed haze spectral attenuations illustrating goodness of fit.

inherent in the computational process are at least an order of magnitude less than those associated with the inability to make a perfect fit of the computed spectral attenuation to the measured spectral attenuation. The average uncertainty which may be attributed to the inferred haze particle size distribution, and the fog drop-size distributions which follow is, in general, less than 10 per cent and does not exceed 20 per cent.

The spectral attenuation labeled "physical measurements" in Fig. 6 of the paper by Arnulf *et al.*, is quite different in shape and magnitude from that labeled "optical measurements." It is this latter spectral attenuation which was used to infer the haze aerosol distribution. Arnulf *et al.* computed the spectral attenuation labeled "physical measurements" from their measured aerosol distributions (Fig. 11 of their paper). The aerosol distribution measured with the "spider web" technique is replotted in Fig. 3 for comparison with that inferred from the optically measured spectral attenuation. The sources of errors associated with the "spider web" technique are well described by Arnulf *et al.* The fact that the smaller particles, that is, those less than about 1.5 μ, are not measurable with the "spider web" is well illustrated in Fig. 3.

3. Fog drop-size distributions

Arnulf *et al.* presented four families of spectral attenuations representing four types of fog; "selective," "evolving fog," "stable fog (1st type)," and "stable fog (2nd type)." The general classification of fog made by Arnulf *et al.*, was based primarily upon the genesis of the fog and the shape of the spectral attenuations. Four spectral attenuations, one for each fog type, are presented in Fig. 4 to illustrate the major differences in the shape of the spectral attenuations resulting from transmission measurements through these fogs. The "goodness of fit" between the computed spectral attenuation and that measured is also depicted in Fig. 4. Four drop-size distributions were synthesized for "stable fog (1st type)," distributions A through D; "stable fog (2nd type)," distributions E through H; and "selective fog" distributions I through J. The twelve fog drop-size distributions are presented in Table 1. The last line of this table lists the specific experimental spectral attenuation curves of Arnulf *et al.* which were approximated by the computed spectral attenuations. The haze distribution is included for comparison. Each quartet of fog drop-size distributions designated by increasing alphabetic symbol, resulted from decreasing optical density. Finally, seven drop-size distributions were synthesized for "evolving fog." These seven distributions, numbered 1 through 7, are discussed in detail because they illustrate the phenomena of droplet growth and fog decay with time.

a) "Stable fog" drop-size distributions. Arnulf *et al.* presented spectral attenuations for "stable fog (1st type" and "stable fog (2nd type)" in Figs. 9 and 10 of

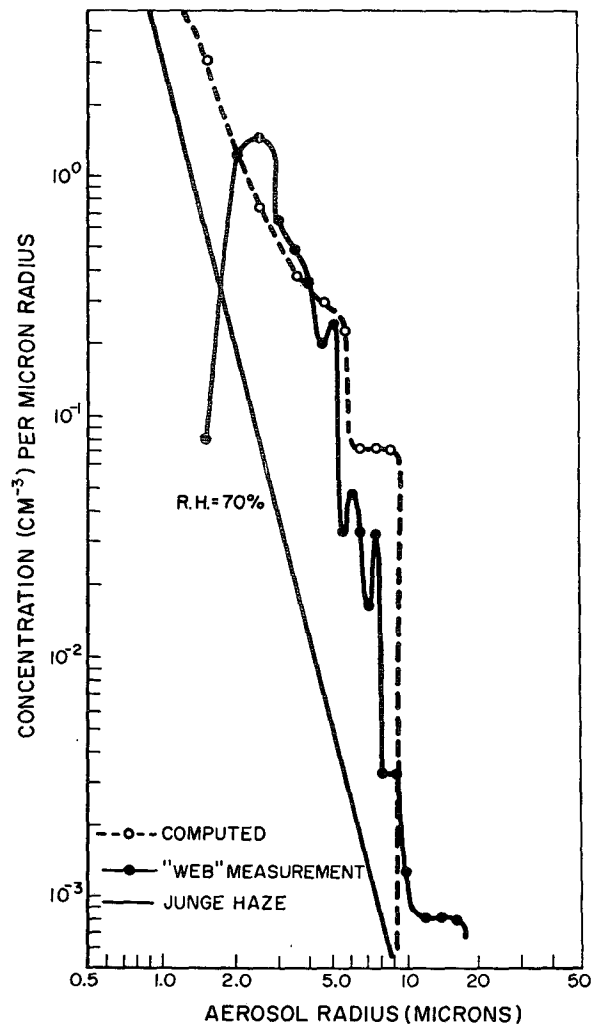

FIG. 3. Comparison of the synthetic haze aerosol distribution with the haze distribution measured with the "spider web" technique.

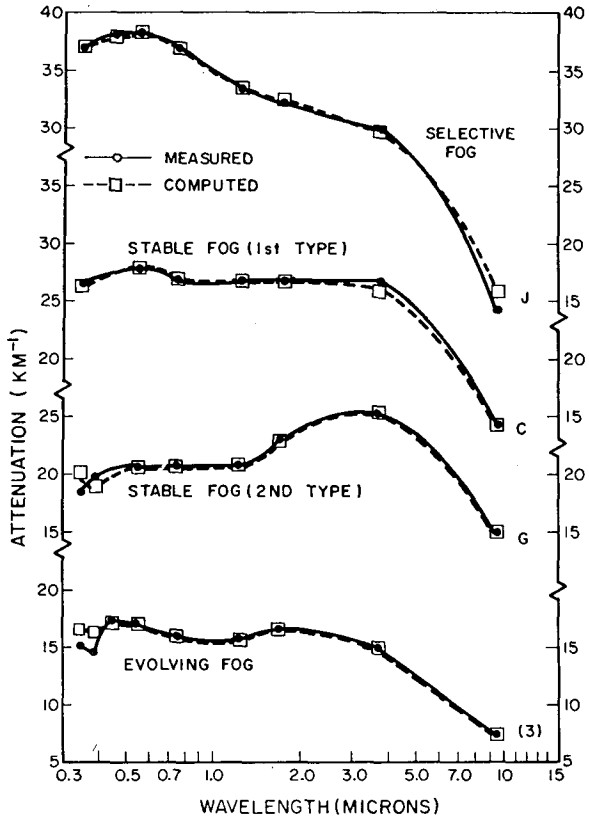

FIG. 4. Measured and computed fog spectral attenuations illustrating goodness of fit.

their paper. Measured spectral attenuations characteristic of "stable fog (1st type)," curve C, and "stable fog (2nd type)," curve G, are shown in Fig. 4 with their computed spectral attenuations. The synthetic stable fog drop-size distributions inferred from the measured spectral attenuations are tabulated in Table 1.

Physical measurements of stable fog drop-size distributions, both of the first and second types, were made by Arnulf *et al.* with the "spider web" technique. Their results, in relative units, are presented in Fig. 11 of their paper. Normalization and conversion of the relative drop-size distributions to the format of this paper allow a comparison of the drop-size distributions inferred from the spectral attenuations with those measured with the "spider web" technique.

Inspection of the eight "stable fog" drop-size distributions indicates that there is considerable variability in the shape of the distributions. However, almost all distributions are at least bimodal in shape, although some are trimodal, and all follow the same general trend. Therefore, all eight stable fog drop-size distributions inferred from spectral attenuations were averaged for comparison with the average drop-size distribution measured with the "spider web" technique. This is illustrated in Fig. 5.

The agreement between the synthetic and the measured stable fog drop-size distributions is reasonably good in the size range of about 1.5 to 8.5 μ radius. Fig. 5 adds credence to the statement of Arnulf *et al.* regarding the inability of the "spider web" to capture a significant number of droplets smaller than 1.5 μ radius. Fig. 5 also illustrates that the optical technique becomes relatively insensitive to changes in distributions for droplets larger than 10 μ radius, whereas the "spider web" technique has good collection efficiencies for the larger size droplets. (Arnulf *et al.* indicated that some coalescence occurs during long exposures; however, this may be offset by the loss of large droplets due to wind vibration.) Comparisons of the drop-size distributions resulting from the two different measuring techniques illustrates rather graphically the size range limitations of both techniques.

b) "*Selective fog*" *drop-size distributions.* Four "selective fog" spectral attenuation curves were selected from Fig. 7 of the paper by Arnulf *et al.* as being representative of that type of fog. The spectral attenuation labeled J in Fig. 4 illustrates the fit of the computed spectral

TABLE 1. Fog drop-size distributions.

Radius (μ)		Concentration of Droplets (cm^{-3})												
		"Stable fog (1st type)"				"Stable fog (2nd type)"				"Selective fog"				
$\bar{r}$	Δr	A	B	C	D	E	F	G	H	I	J	K	L	Haze
0.35	0.1	...	...	...	1040	...	...	...	...	...	...	8180	2510	1115
0.45	0.1	4190	4930	2420	525	1360	...	...	451	9200	5870	1240	1880	751
0.75	0.5	1410	493	120	316	394	511	577	451	738	1170	818	188	18.9
1.5	1.0	207	...	46.2	105	...	102	46.2	45.1	296	97	124	54.4	3.2
2.5	↑	70.2	49.3	24.1	31	39.4	128	161	134	74	48.5	6.3	6.3	0.75
3.5	|	70.2	99.2	46.2	21	136	51	...	...	36.6	48.5	21.4	7.5	0.38
4.5	|	105	99.2	46.2	16	117	51	...	17.2	74	97	10.3	1.3	0.30
5.5	|	70.2	49.3	35.2	16	19.6	26	...	8.2	74	19.6	...	2.5	0.23
6.5	|	35.1	...	12.1	...	10	10	23.3	4.5	7.4	9.7	...	...	0.08
7.5	↓	17.3	...	...	...	4	10	11.5	...	...	9.7	...	...	0.08
8.5	1.0	...	...	...	...	...	...	...	...	...	...	...	...	0.08
Total (cm^{-3})		6175	5720	2750	2070	2080	889	819	1110	10,500	7370	10,400	4650	1890
Fig. (Cur.)*		9(2)	9(9)	9(11)	9(17)	10(2)	10(4)	10(10)	10(14)	7(2)	7(4)	7(5)	7(7)	6(AV)

* Fig. (Cur.) refers to the figure numbers and curves, counting from top to bottom, in the study of Arnulf *et al.* (1957); AV refers to average values.

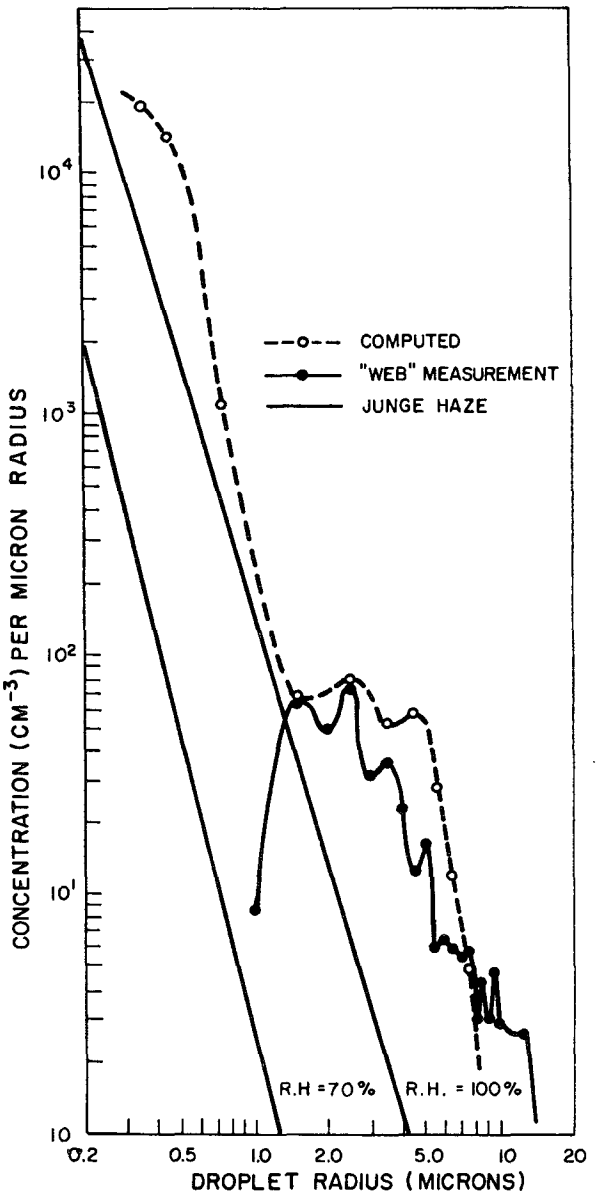

FIG. 5. Comparison of the average synthetic "stable fog" drop-size distribution with "stable fog" distribution measured with the "spider web" technique.

attenuation resulting from the synthetic drop-size distribution with that measured by Arnulf *et al.* The four "selective fog" drop-size distributions I through L, are included in Table 1.

These four "selective fog" drop-size distributions, though varying in concentration, are all bimodal in shape and follow the same general trend. No comparison can be made between the synthetic "selective fog" drop-size distributions and a measured "selective fog" distributions, because Arnulf *et al.* apparently were unable to obtain a significant sample of aerosols with the "spider web" technique. The only basis for this assumption is that "selective fogs" appears to have a high concentration of small droplets and are more transient than "stable fogs." However, the "selective fog" drop-size distributions all exhibit a bimodal shape which is very similar to the shape predicted by theory.

Using droplet growth theory, Neiburger and Chien (1960) computed drop-size distributions as a function of time after the initiation of the droplet growth process. The average of their stratus A and stratus B drop-size distributions resulting after 49 min of growth is plotted in Fig. 6 with the average "selective fog" drop-size

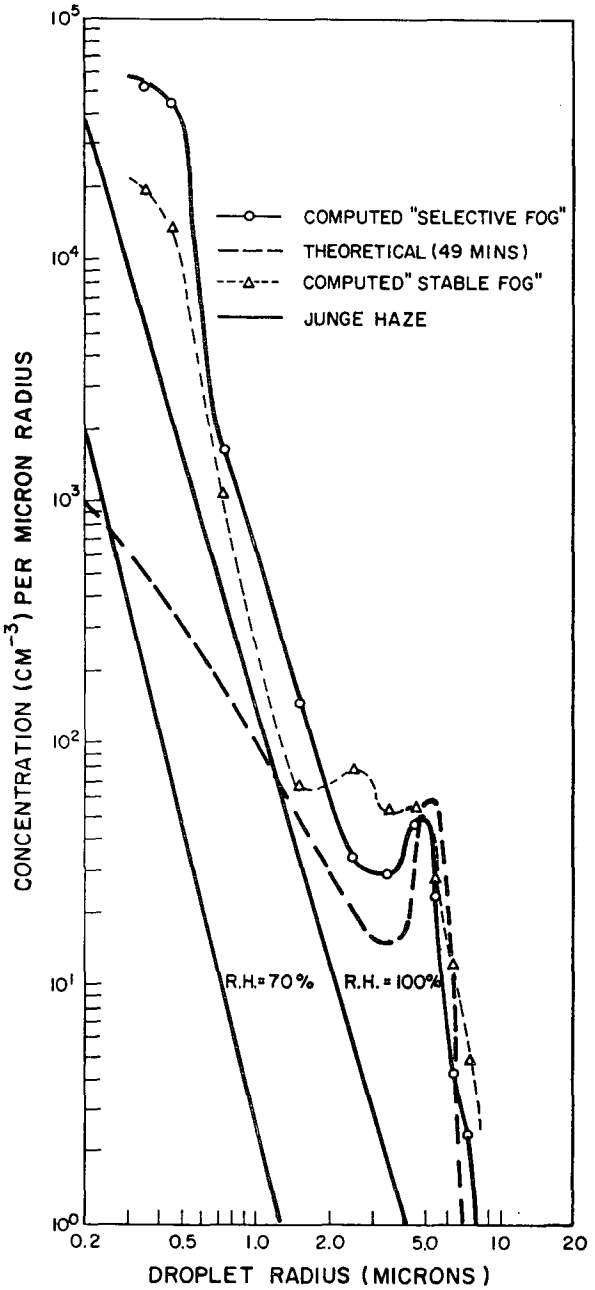

FIG. 6. Comparison of the average synthetic "selective fog" drop-size distribution with a theoretical distribution and the average "stable fog" distribution.

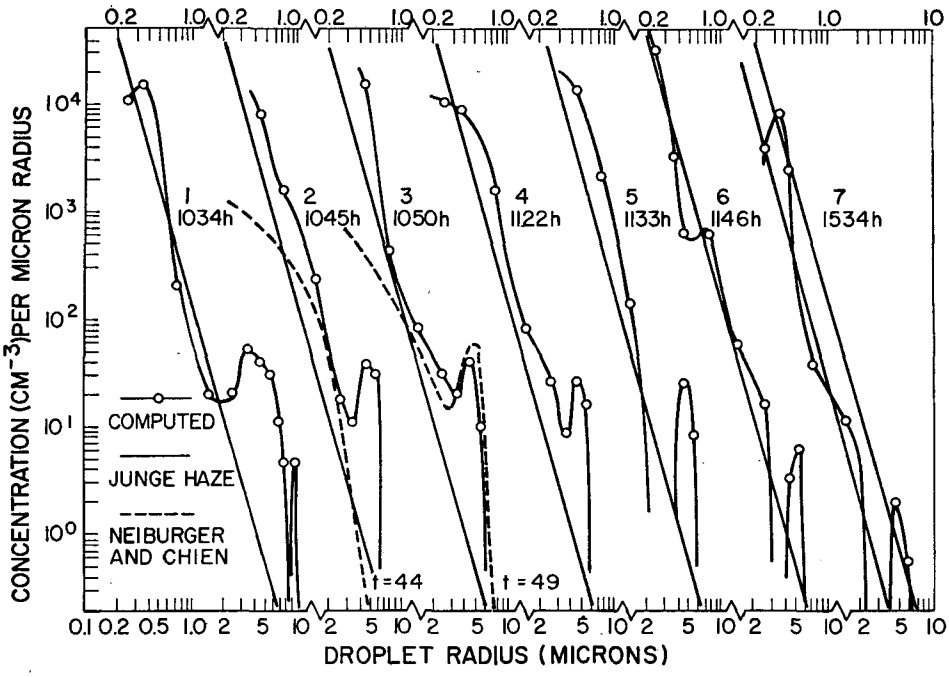

FIG. 7. Time-phased "evolving fog" drop-size distributions illustrating droplet growth and fog dissipation.

distribution. The reasonably good agreement between the theoretical distribution and that inferred from spectral attenuations suggests that droplet growth theory can at least be used to predict "selective fog" drop-size distributions. The average "stable fog" drop-size distribution is also plotted in Fig. 6 for comparison with the average "selective fog" distribution.

c) "Evolving fog" drop-size distribution. Seven "evolving fog" spectral attenuations were selected from Fig. 8 of the paper by Arnulf *et al.* for analysis because they represent the dissipation of fog over a period of five hours. A representative spectral attenuation, curve 3, is plotted in Fig. 4 to illustrate the general shape and goodness of fit of the computed spectral attenuation with that measured. The seven "evolving fog" drop-size distributions are plotted in Fig. 7 with the Junge haze in an environment of 100 per cent relative humidity.

Neiburger and Chien (1960) computed drop-size distributions as a function of time after the initiation of the droplet growth process. Their study also shows that droplet growth proceeds at a near regular rate as the relative humidity approaches saturation. As saturation and supersaturation occurs, the growth process is accelerated. Thereafter, the droplet growth continues in a regular manner in an environment containing a few tenths of a per cent supersaturation.

The most rapid growth is illustrated by a 0.2 μ radius aerosol which grows to 12 μ radius during the 100 min growth life period. During the accelerated growth period, from the 42nd to the 50th minute, the original 0.2 μ radius aerosol grows from 0.3 to 5.0 μ radius in 8 min. Thus, 39.8 per cent of the droplet's growth in size and 7.2 per cent of its growth in volume occur during only 8 per cent of the selected growth period of 100 min.

The time dependent drop-size distributions computed by Neiburger and Chien are monomodal until after about 47 min have elapsed. At that time, the distributions become bimodal. The first maximum of a multimodal distribution is that occurring in the original aerosol distribution at about 0.02 μ radius. Therefore, the drop-size distributions presented by Neiburger and Chien are only bimodal distributions; yet, three of the seven "evolving fog" distribution in Fig. 7 are at least trimodal. The occurrence of multimodal distributions is not necessarily inconsistent with the droplet growth theory if it is assumed that air parcels containing droplets at different stages of growth are being mixed by mild turbulence. The mixing must be gentle enough to preserve the cloud or fog; otherwise, dryer air from outside will be entrained resulting in the evaporation of some droplets.

If the above considerations are applied to the "evolving fog" distributions of Fig. 7, which are summarized in terms of their physical properties in Table 2, some general statements are possible.

At 1034 hours, a well-developed but dissipating fog has been in existence for some time as indicated by the presence of a significant number of 9.5 μ radius droplets. However, the existence of a sub-micron maximum in concentration at 0.35 μ radius indicates the recurrence of the growth process. By 1045 there is a significant increase in concentration of sub-micron and micron size droplets inferring the continued growth of the sub-

TABLE 2. "Evolving fog" characteristics.

Distribution No.	Time (hours)	Concentration (cm^{-3})	Liquid water content (gm m^{-3})	Secondary modal (μ)	Visibility (km)
1	1034	2910	0.073	3.5	0.14
2	1045	1970	0.048	4.5	0.16
3	1050	2050	0.032	4.5	0.23
4	1122	2960	0.030	4.5	0.21
5	1133	2020	0.020	4.5	0.29
6	1145	4320	0.009	5.5	0.59
7	1534	1530	0.0013	4.5	1.70

micron aerosols. The secondary modal maximum concentration of droplets at 3.5 μ radius has now shifted to 4.5 μ radius. The drop-size distribution, according to Neiburger and Chien, resulting after 44 min of the growth process, is plotted for comparison with the "evolving fog" distribution occurring at 1045.

Five minutes later the "evolving fog" distribution is well approximated in the micron size range by the Neiburger and Chien's drop-size distribution resulting after 49 min of growth. There is also a suggestion of new sub-micron growth which would be necessary if the fog is to persist.

As time progresses, the sub-micron droplet growth periodically occurs to sustain the fog even though the fog has been dissipating slowly since the beginning of the spectral attenuation measurements. This is evidenced by the steady decrease in liquid water content and the increase in visibility. By 1146 hours, there is no further growth of sub-micron aerosols and the secondary modal maximum in concentration has decreased and shifted to 5.5 μ radius. By 1534 the "evolving fog" has almost completely degenerated into a dense haze. The droplet spectrum migrates between the two Junge haze distributions in environments of 99 and 100 per cent relative humidity.

In postscript, it must be noted that at 1534 there is again a recurrence of the increase in sub-micron aerosols which may be indicative of the reformation of fog. As a matter of fact, Arnulf *et al.* made one more spectral attenuation measurement at 1722 in a dense fog with a visibility of about 0.2 km.

4. Discussion of aerosol distributions

In general, the concentration of droplets between 0.3 and 2.0 μ radius is about 50 times more than a Junge haze in a saturated environment. Between 2.0 and about 10 μ radius, the concentration may vary from 50 to 500 times more than the haze concentration depending upon the size of droplets being considered. This generalization is evident in Fig. 6, but inspection of the individual droplet distributions illustrates that no two distributions are alike in detail. It is doubtful if all of the spectral attenuations presented by Arnulf *et al.* were analyzed, that two identical drop-size distributions would result. However, there are similarities and characteristics which are worthy of comment.

The 20 drop-size distributions presented in this paper have been summarized in Table 3 in terms of their general description, total number of droplets, liquid water content for droplets ranging in size from about 0.3 to 10.0 μ radius, and the visibility determined from the optical density at a wavelength of 0.55 μ. (The visibility derived from the measured optical density at a specific wavelength is the analog of the visibility computed

TABLE 3. Summary of aerosol distributions.

Type of obstruction	Distribution designation	Concentration (cm^{-3})	Concentration uncertainty (per cent)	Liquid water content (gm m^{-3})	Visibility (km)
Dense haze	—	1890	6.8	0.0014	1.18
Stable fog (1st type)	A	6175	0.4	0.183	0.062
	B	5720	0.3	0.095	0.099
	C	2750	0.8	0.070	0.141
	D	2070	3.1	0.025	0.283
Stable fog (2nd type)	E	2080	1.1	0.105	0.099
	F	889	0.6	0.087	0.125
	G	819	1.4	0.060	0.189
	H	1110	2.3	0.028	0.260
Selective fog	I	10,500	1.1	0.108	0.067
	J	7370	1.1	0.097	0.103
	K	10,400	4.7	0.013	0.208
	L	4650	5.6	0.006	0.376
Evolving fog	1	2910	0.6	0.073	0.142
	2	1970	4.0	0.049	0.163
	3	2050	2.7	0.032	0.230
	4	2960	2.7	0.030	0.211
	5	2200	2.7	0.020	0.290
	6	4320	4.0	0.009	0.588
	7	1530	5.3	0.0013	1.70

with Koschmieder's formula at that wavelength.) The uncertainty in the total number of droplets due to fitting the computed spectral attenuation derived from the synthetic distribution of aerosols to the measured spectral attenuation, is also included. The average uncertainty in concentration of all 20 distributions is 2.6 per cent.

In selecting the spectral attenuation curves to be analyzed, it was stated that decreasing optical density curves were chosen for each type of fog. It may be noted in Table 3 that within each fog classification the liquid water content decreases as the visibility increases. This relationship is further illustrated in Fig. 8 where the visibility for each distribution is plotted as a function of the liquid water content. All of the "stable fog" and "evolving fog" data can be represented by the empirical formula

$$V = 0.024w^{-0.65}, \tag{2}$$

where V is the visibility in km and w is the liquid water content in gm m^{-3}. The "selective fog" and the dense haze appear to be more nearly represented by Eq. (2) when the constant 0.024 is replaced with 0.017.

The major difference between Eq. (2) and Trabert's (1901) formula is that the latter is dependent upon the determination of a volumetric median droplet size which is assumed to be representative of the drop-size distribution. The validity of Trabert's formual has been questioned by aufm Kampe and Weickmann (1952) on the basis that the constant varies with the character of the droplet spectrum. The liquid water content used in Eq. (2) is inherently dependent upon the droplet spectrum because it is computed from the drop-size distribution. Therefore, this equation is valid for measured liquid water contents which excludes aerosols larger than 10 μ (which may be relatively few in number) and smaller than 0.3 μ radius (which contribute a relatively insignificant amount of liquid water to the total water content).

A possible explanation and justification for the existence of two different constants in the relationships of visibility and liquid water content may be dependent upon the type of fog involved. The "evolving fog" and "stable fog" are well-developed fogs which apparently have been in existence for sometime, whereas the "selective fog" appears to be newly formed by condensation on haze aerosols. In general, the ratio of the concentration of sub-micron aerosols to micron size aerosols is greater for dense haze and "selective fog" than for "stable" and "evolving fog." Therefore, it is suggested that Eq. (2) is valid for well-developed older or dissipating fogs and that the substitution of the smaller constant is more appropriate for newly forming fogs.

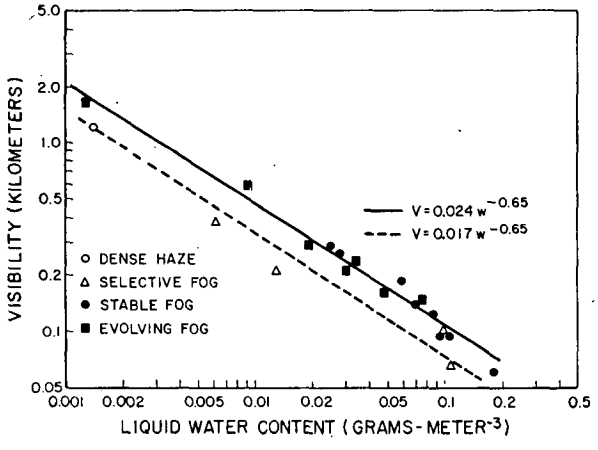

FIG. 8. Correlation of liquid water contents and visibilities with Eq. (2).

The relationship between liquid water content and visibility expressed by Eq. (2) evolved from a limited amount of data. Additional data is being assimilated and subjected to an objective analysis. It appears at this time that there will be no significant change in the coefficients of Eq. (2) for the well-developed stable fog. However, additional data pertaining to newly formed developing fog indicates that the coefficients must be modified (but not the form of the equation), because the data diverges from that predicted by Eq. (2) at reduced visibilities.

All 19 of the fog drop-size distributions presented in this paper are at least bimodal distributions. Many are trimodal. The bimodal characteristics of drop-size distributions were first presented by Eldridge (1957a) for the case of cumulus type clouds being formed by orographic lifting over the summit of Mt. Washington. Stewart (1957) found multimodal aerosol distributions in fogs in England. The existence of multimodal drop-size distributions in developing fog and clouds appears to be a true characteristic of the distributions. If it is assumed that droplet growth, from nuclei to fog or cloud droplets, proceeds in much the same manner for both fog and clouds, then the theoretical basis for bimodal distributions may be found in the paper by Neiburger and Chien (1960).

Considering the dynamic nature of the type of atmosphere necessary to support droplet growth, which must include some intermixing, it would be quite fortuitious to find a measured aerosol distribution following the theoretical model exactly. Yet, there is a remarkable resemblance between the average "selective fog" and the third "evolving fog" drop-size distributions and that predicted after 49 min of growth for a stratus cloud by Neiburger and Chien.

Inspection of the family of drop-size distributions presented by Neiburger and Chien leads one to speculate that the drop-size distributions presented in this paper exhibit both growth and degeneration of droplets within different size intervals. Some portions of the droplet distribution appear to be growing, while other droplets are evaporating. Certainly, the dynamic nature of the atmosphere admits the possibility of this situation on the microscale of phenomena. Because clouds and fog form, persist for some time, and eventually dissipate,

it seems reasonable to postulate a life history of fogs and clouds in terms of varying time dependent drop-size distributions.

5. Epilogue

The relationship between visibility and liquid water content expressed above may be considered a "rediscovery of science." Houghton (1939) has inferred such a relationship from his continuous records of visibility and liquid water content. He further indicated that the visibility was related to the liquid water content raised to the 0.6 power. He then argued that the exponent would be 2/3 if the concentration of droplets is constant rather than the size, but concluded that no absolutely fixed relationship between visibility and liquid water content exists because the exponent varied from 0.4 to 0.8.

In this paper, variations of the drop-size distributions are limited to two model-like droplet spectra, those characteristic of a developing fog and a stable fog. Therefore, the relationship between the visibility and the liquid water content, as expressed by the form of Eq. (2), is dependent upon changes in the droplet concentration and is independent of the droplet spectrum except for the two general classifications of the fog.

REFERENCES

Arnulf, A., J. Bricard, E. Curé and C. Véret, 1957: Transmission by haze and fog in the spectral region 0.35 to 10 microns. *J. Opt. Soc. Amer.*, **47**, 491–498.

aufm Kampe, H. J., and H. K. Weickmann, 1952: Trabert's formula and the determination of the water content in clouds. *J. Meteor.*, **9**, 167–171.

Eldridge, R. G., 1957a: Measurements of cloud drop-size distributions. *J. Meteor.*, **14**, 55–59.

——, 1957b: Reply. *J. Meteor.*, **14**, 575–577.

Gibbons, M. G., 1958: Wavelength dependence of the scattering coefficient for infrared radiation in natural haze. *J. Opt. Soc. Amer.*, **48**, 172–176.

Houghton, H. G., 1939: On the relationship between visibility and the constitution of clouds and fog. *J. Aero. Sci.*, **6**, 408–411.

——, and W. R. Chalker, 1949: The scattering cross sections of water drops in air for visible light. *J. Opt. Soc. Amer.*, **39**, 955–957.

Johnson, J. C., and J. R. Terrell, 1955: Transmission cross sections for water spheres illuminated by infrared radiation. *J. Opt. Soc. Amer.*, **45**, 451–454.

Junge, C., 1955: The size distribution and aging of natural aerosols as determined from electrical and optical data of the atmosphere. *J. Meteor.*, **12**, 13–25.

——, 1957: Atmospheric composition. *Handbook of Geophysics for Air Force Designers*, Bedford, Geophysics Research Directorate, U. S. Air Force, 8.6–8.12.

Neiburger, M., and C. W. Chien, 1960: Computations of the growth of cloud drops by condensation using an electronic digital computer. *Physics of Precipitation*, Geophys. Monogr. No. 5, Washington, D. C., Amer. Geophys. Union, 191–210.

Penndorf, R., 1957: Comments on measurements of cloud drop size distributions. *J. Meteor.*, **14**, 573–574.

Stewart, K. H., 1957: Some observations on the composition of fogs. A meteorological paper of the Meteorological Research Committee (London), MRP No. 1074, 12 pp.

Trabert, W., 1901: Die Extintion des Lichtes in einem truben Medium (Sichtweite in Wolken). *Meteor. Z.*, **18**, 518–525.